A time dependent Model for the activation of COMPTEL

Martin Varendorff*, Uwe Oberlack*, Georg Weidenspointner*, Roland Diehl*, Rob van Dijk†, Marc McConnell†† and James Ryan††

*Max-Planck-Institut für extraterrestrische Physik, D-85740 Garching, Germany
†ESTEC, Space Science Department, Keplerlaan 1, NL-2201 AZ NOOrdwijk, Netherlands
††University of New Hampshire, Morse Hall, Durham, N. H., 03824, USA

Abstract. The structure of the CGRO satellite is irradiated by cosmic rays and trapped particles from radiation belts. These incident particles produce radioactive nuclei in nuclear reactions with the satellite structure. Most of the radiation dose can be attributed to the passages through the South Atlantic Anomaly. The incident particle flux on the COMPTEL instrument is estimated from the event rate of a plastic scintillation detector. This event rate is modeled with a Neural Network simulation. The increase of the event rate during SAA passages is taken as a measure for the amount of induced radioactivity. A Neural Network Model is used to derive the buildup of radioactive nuclei in the instrument over the first five years of the mission. Measurements of the internal ^{22}Na- and ^{24}Na-activity are used to estimate the proton flux in the SAA. The result is consistent with earlier measurements and models.

INTRODUCTION

Instrument:
A detailed description of COMPTEL onboard CGRO can be found in Schönfelder et al. (1993). COMPTEL consists of two detector modules. An incoming gamma-ray photon is Compton scattered in the upper D1 detector (liquid scintillator) and totally absorbed in the lower D2 detector (NaJ). Two calibration units ("Cal-units") are located between the two detection layers at the side of the instrument opposite to each other (Snelling et al., 1986). The detector inside a Cal-unit is comprised of a ^{60}Co doped plastic scintillation wafer, viewed by two 1/2 inch PMTs. The primary use of the Cal-unit is to tag the gamma-rays from the decay of ^{60}Co.
Input data:
The count rate of the plastic scintillator inside Cal-unit B varies considerably

with respect to several parameters. The left plot in Figure 1 shows the variation of the count rate with time. The effect of the satellite reboost around TJD 9300 from about 330 km above earth to about 440 km is clearly visible. The dependance on solar cycle is shown in the right part of Figure 1. The gray dots represent measurements at the beginning of the mission around solar maximum; the black dots, near solar minimum in the same altitude range.

Neural Network Simulation:

A Neural Network Simulation was chosen to model the count rate as a function of the orbital parameters, because most of the functional dependencies are unknown and because the parameter space is unevenly filled. Measurement noise and data gaps prevent use of the data itself as an activation measure. A Neural Network Simulation Model with 7 input neurons, and 2 hidden layers à 10 Neurons and one output neuron was built. The activation $o_{(j,n)}$ of the neuron j in layer n equals the sigmoidal function F of the weighted sum of the activation from all N neurons in layer n-1 plus a bias b_j:

$$o_{(j,n)} = F\left(\sum_{i=1}^{N(n-1)} w_{ij} \cdot o_{(i,n-1)} + b_j \right), \qquad \text{with} \qquad F(x) = \frac{1}{1+e^{-x}}$$

Each input neuron presents one of the seven input parameters as its activation to the network. The input values are propagated through the network using the above-mentioned formulas. The output of the last neuron represents the model value corresponding to the input values. The following model parameters were chosen: height above earth, geographic longitude and latitude, time since launch (to include solar cycle variations), and the orientation of the satellite relative to the propagation direction (azimuth, declination), to account for asymmetries in the incoming particle flux. To take care of the discontinuity of the azimuth angle at 360°/0°, the sine and the cosine of this angle are used as input parameters. During the training of the network using the backpropagation algorithm, the weights w_{ij} and the biases b_j are optimized, minimizing the deviation between model and data. A similar approach was made for the Neural Network simulation of the background count rate of

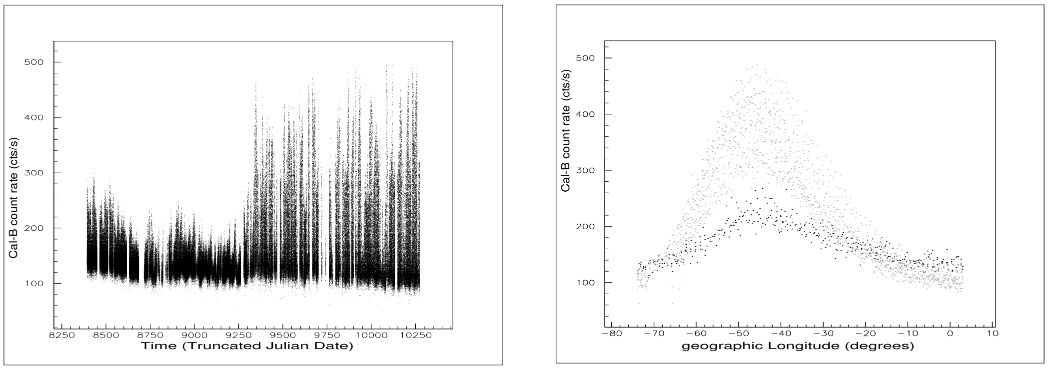

FIGURE 1. Measured count rates as a function of time and orbital parameters.

COMPTEL (Varendorff et al., 1996).

Measurement of the cascade lines:
At the decay of ^{22}Na a 1.275 MeV photon and β^+-particle are emitted simultaneously. The annihilation of the positron (after its deceleration) produces two 511 keV photons moving in opposite directions. One of the 511 keV photons may hit the upper detector (D1), while the 1.275 MeV photon (from the same original decay) hits the lower detector (D2). The complementary process (1.3 MeV photon in D1, 511 keV photon in D2) is not detected due to the threshold of the D2 detector (650 keV). The measured apparent time of flight of such an event is only slightly smaller than the time of flight of a photon which is Compton scattered in D1 and absorbed in D2. After the decay of ^{24}Na a photon at 1.369 MeV and a photon at 2.754 MeV are emitted simultaneously. A detailed description of the fitting of the cascade lines (^{22}Na and ^{24}Na) can be found in Oberlack et al., 1997.

RESULTS

Model data comparison:
A comparison of the measurement of the activation of the COMPTEL instrument and the model is shown in Figure 2 (each dot represents one observation period). The scaling factor from the measured Cal-unit count rates to the number of ^{22}Na- and ^{24}Na-nuclei as well as the initial number of those nuclei are taken from a fit of the model to the measured data. The scatter in ^{22}Na is caused by the statistical and systematic error of the fit to the data. The activition in ^{24}Na with a half life time of only 15 hours shows much more scatter than the activation in ^{22}Na. This is caused by the different orientations of the satellite relative to the anisotropic incident particle flux. The strong increase of the cascade lines after reboost around TJD 9300 is clearly visible in both plots. The recent reboost to a hight of about 517 km will increase the

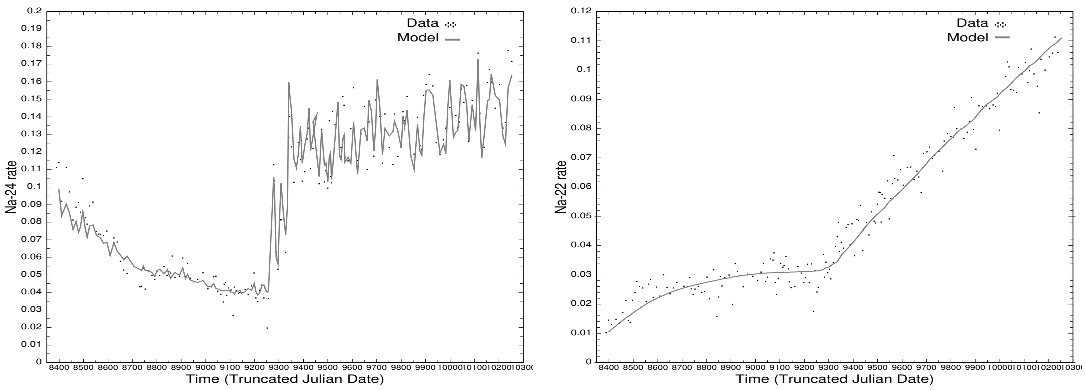

FIGURE 2. Comparison of the measured ^{24}Na- (left) and ^{22}Na-activity (right) with the predicted values from the Neural Network Model.

combined background from ^{22}Na and ^{24}Na by a factor of 2 to 3 in the next 1 to 2 years.

Estimation of the average incident proton flux:

The radioactive isotope ^{22}Na is produced by the interaction of energetic protons with Al-atoms of the structure of the satellite. The measured time of flight distribution of the events from the ^{22}Na decay shows, that mainly events from the structure near the upper detector (D1) contribute to the signal. The Al-mass around D1 is approximately 125 kg with a thickness in the range of 1 cm to 2 cm. The average daily proton fluence is then estimated by comparing the daily increase in the number of proton produced nuclei with an estimate of the efficiency of the production of these nuclei by protons. To simplify the calculation, all the Al mass was put in a plate of 2 cm thickness and irradiated by protons following the spectral shape of a model calculation of the orbital proton spectrum (Stassinopoulos, 1981). At the beginning of the mission during solar maximum at an orbital altitude of 440 km a daily production of $1.7 \cdot 10^7$ nuclei of ^{22}Na was derived from measurements of the ^{22}Na count rate. A daily proton fluence ($E > 100$ MeV) of $2.3 \cdot 10^5$ protons/cm^2 can be inferred from those numbers. For an altitude of 462 km a daily fluence of $5 \cdot 10^5$ protons/cm^2 was predicted by Dyer et al. (1994).

Acknowledgements

We would like to thank the MITRE Corporation for providing the Aspirin/MIGRAINES software package. The COMPTEL project is supported by the German government through DARA grant 50 QV 90968, by NASA under contract NASS-26645 and by the Netherlands Organisation for Scientific Research (NWO).

REFERENCES

1. Schönfelder, V., Aarts, H., Bennett, K., et al., 1993, Astrophysical Journal Suppl. **86**, 657.
2. Snelling, M., et al., 1986, Nuclear Instruments & Methods, **A248**, 545-549
3. Oberlack, U., et al., "A New Background Model for COMPTEL 1.8 MeV Data", these Proceedings, Poster 20-5.
4. Varendorff, M., Forrest, D., McConnell, M., and Ryan, J., 1996, A&A Suppl., **120**, 699-702.
5. Stassinopoulos, E. G., "GRO charged particle radiation study", NASA Report X-601-81-38, Table 3.
6. Dyer, C. S., Truscott, P. R., Evans, H. E., Hammond, N., Comber, C., Battersby, S., 1994, IEEE Transactions on Nuclear Science, Vol. **3**, 438.